Applied Thermal Engineering 71 (2014) 56–61

Contents lists available at ScienceDirect

Applied Thermal Engineering

journal homepage: www.elsevier.com/locate/apthermeng

Ultrafast thermalization dynamics of gold-coated fused silica irradiated by a femtosecond laser

Yanmin Wu, Feng Chen*, Guangqing Du*, Qing Yang, Yan Ou, Hao Bian, Jinhai Si, Xun Hou

State Key Laboratory for Manufacturing Systems Engineering & Key Laboratory of Photonics Technology for Information, School of Electronics & Information Engineering, Xi'an Jiaotong University, 710049, China

HIGHLIGHTS

- The ultrafast temperature fields is predicted by FEM simulations.
- The critical thickness for gold-coated fused silica is obtained.
- The effect of gold layer thickness on thermalization of gold-coated fused silica is explored.

ARTICLE INFO

Article history:
Received 7 November 2013
Accepted 8 June 2014
Available online 25 June 2014

Keywords:
Gold-coated fused silica
Ultrafast thermalization dynamics
Femtosecond laser
Thermal relaxation model

ABSTRACT

The ultrafast thermalization dynamics in gold-coated fused silica irradiated by femtosecond laser are numerically investigated by Finite Element Method (FEM). The temporally sequential thermal relaxation model, which jointly considers the two temperature relaxation and the thermal diffusion relaxation dynamics is proposed for explaining the thermalization characteristics in gold-coated fused silica system. It is revealed that the gold layer thickness of 0.6 μm is the critical thickness for influencing the temperature distribution across gold-coated fused silica system. In addition, the effect of gold layer thickness on thermalization dynamics of gold-coated fused silica system is examined in detail.

1. Introduction

Femtosecond laser has the capability of non-thermal processing due to ultrashort pulse durations and ultrahigh power densities, which can greatly minimize the thermal damage and considerably increase the fabrication precision and quality [1,2]. The potential advantages of femtosecond laser processing of material originate from the non-equilibrium process in material, in which electrons and phonons can be considered as respective systems. Many previous researchers have investigated the thermal dynamics process in metal based on the two temperature model. The ablation characteristics of Au, Ag, and Cu metals using a femtosecond laser were investigated by Furusawa et al. [3]. Chen et al. used an axisymmetric, dual-hyperbolic, two-temperature model to investigate the thermal response of ultrashort laser pulse interaction with a metal film [4]. However, most of them treated the gold film as free-standing one, which becomes even incorrect for multilayer substrate system as the thermal relaxation period exceeds the electron-phonon relaxation cycle.

Multilayer structure and multiple interfaces are playing an important role in electronic device interconnect and packaging in microelectronics industry. The theoretical researches about the heat transfer mechanism of packaging material and packaging material failure mechanism are still limited for far. Many previous studies on thermal dynamics in metal-coated substrate system with ultrashort laser pulse excitation are focused on interface thermal dynamics. The phonon transmission characteristic across solid-solid interface was studied by Swartz and Pohl [5]. Then Hopkins et al. studied the influence of substrate on electron–phonon coupling measurements in thin gold films [6,7]. Recently, Guo et al. employed transient thermal reflectance (TTR) techniques to investigate the interface heat transfer in thin gold films on silicon substrates [8]. They concluded that it is possible to isolate the effect of direct electron-phonon coupling across the interface due to the strong non-equilibrium between electrons and phonons during ultrafast laser excitation. When the thermal dynamics process in the metal-coated substrate system goes beyond the electron-phonon coupling period [9,12,13], the isolation of

* Corresponding authors.
E-mail addresses: chenfeng@mail.xjtu.edu.cn (F. Chen), guangqingdu@mail.xjtu.edu.cn (G. Du).

http://dx.doi.org/10.1016/j.applthermaleng.2014.06.011
1359-4311/

electron-phonon coupling with the substrate will lead to incorrect conclusions. Therefore, it is necessary to investigate the basic mechanism of full thermalization processes in gold layer-substrate system beyond electron-phonon coupling cycle for well optimizing the micro-fabrication processes.

In this paper, we propose a temporally sequential thermal relaxation model, which jointly considers the sequential processes of two temperature relaxation and thermal diffusion relaxation for investigation of the ultrafast thermalization dynamics in gold-coated fused silica system. The electron and phonon temperature field distributions along the depth of gold-coated fused silica at different delay time beyond the electron-phonon coupling process are analyzed. The dependence of temperature distribution of gold-coated fused silica on laser parameters and gold layer thickness are explored carefully. Moreover, the effect of fused silica substrate on temperature field distribution of gold-coated fused silica system is examined in detail.

2. Modeling and methods

For gold-coated fused silica system, the thermal relaxation process becomes significantly distinct during different thermal relaxation periods. It is widely accepted that the well-known two-temperature relaxation dominates in the electron-phonon relaxation period on picosecond timescale [14–18]. However, after the two temperature relaxation, the normal thermal diffusion will take place across the interface between gold layer and fused silica substrate. Therefore, it is very important to take the full thermal diffusion processes into account for well describing ultrafast thermal excitation dynamics in the gold-coated fused silica system. The gold-coated fused silica system is shown in Fig. 1. The laser is incident from the left. In the current studies, the fused silica substrate is taken as bulk target. It means that the less thermal energy can reach the bottom of fused silica substrate. On the other hand, the gold layer thickness is treated as optional parameter in the simulations in order to explore the dynamics process of gold thickness effect on the ultrafast thermalization of gold-coated fused silica system.

2.1. The temporally sequential thermal relaxation model

The proposed temporally sequential thermal relaxation model jointly considers the full thermal relaxation processes including the two-temperature relaxation and thermal diffusion relaxation in order to explore ultrafast thermalization dynamics of gold-coated fused silica system irradiated by a femtosecond laser pulse. Because of the symmetry of Gaussian laser spot, it is reasonable to simplify the model into one dimensional (1-D) form. Herein, building the 1-D model is not only convenient to get fundamental understanding of thermal relaxation dynamics in gold-coated fused silica system, but also saves computering time largely. For the 1-D gold-coated fused silica system, the proposed model is described as follows:

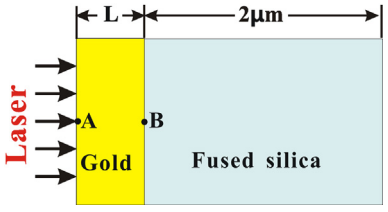

Fig. 1. The schematic of gold-coated fused silica system. The thickness of gold layer is L. The thickness of fused silica is 2 μm. (For interpretation of the references to color in this figure legend, the reader is referred to the web version of this article.)

$$C_e\frac{\partial T_e^I}{\partial t}=\frac{\partial}{\partial x}\left(k_e^I\frac{\partial T_e^I}{\partial x}\right)-g\left(T_e^I-T_p^I\right)+Q \tag{1}$$

$$C_p^I\frac{\partial T_p^I}{\partial t}=\frac{\partial}{\partial x}\left(k_p^I\frac{\partial T_p^I}{\partial x}\right)+g\left(T_e^I-T_p^I\right) \tag{2}$$

$$C^{II}\frac{\partial T^{II}}{\partial t}=\frac{\partial}{\partial x}\left(k^{II}\frac{\partial T^{II}}{\partial x}\right) \tag{3}$$

Eqs. (1) and (2) describe the laser energy deposition and the following two temperature relaxation in gold layer. After the two temperature relaxation termination, the electron-phonon coupling mechanism disappears in gold film due to the establishing of the thermal equilibrium between electrons and phonons system. Therefore, the Fourier thermal diffusion relaxation is represented by and Eq. (3). The subscripts e and p refer to the electron and phonon parameters. $C=C_{e0}\,(T_e/T_0)$ is the temperature-dependent electron heat capacity; C_p is the phonon thermal capacity which can be considered as a constant. T_e is the electron temperature; T_p is the phonon temperature. $k_e=k_0\,(T_e/T_p)$ is the temperature-dependent electron heat conductivity; the phonon heat conductivity is normally neglected in the two-temperature relaxation period due to the quite longer phonon diffusion compared to the electron-phonon relaxation time. g is the electron-phonon coupling coefficient [19,20].

Besides the electron and phonon parameters, t is the time; x is the depth; T_0 is the room temperature. Q is the energy absorption rate, which can be written as:

$$Q=S\times U(t) \tag{4}$$

Q can be modeled with a Gaussian temporal profile [21,22] (In the temporally sequential thermal relaxation model, the Gaussian temporal profile is simplified to 1-D form due to the symmetry of Gaussian laser spot).Where

$$S=\sqrt{\frac{4\ln 2}{\pi}}\,\frac{1-R}{t_p\alpha}F\times\exp\left(-\frac{x}{a}\right) \tag{5}$$

$U(t)$ represents the temporal energy absorption rate:

$$U(t)=\exp\left[-4\ln 2\left(\frac{t-2t_p}{t_p}\right)^2\right] \tag{6}$$

here, R is the target reflection coefficient; t_p is the full width at half maximum (FWHM) with linear polarization. The effective optical penetration depth can be written as the simple form of $\alpha=\delta+\delta_b$, $\delta=15.3$ nm is the optical penetration depth, $\delta_b=100$ nm is the ballistic length for gold film [9–11]. F is the laser incident energy.

2.2. Initial and boundary conditions

The calculation starts at the time $t=0$ and the initial conditions for both electrons and phonons are assumed to be room temperature. Thus

$$T_e(x,0)=T_p(x,0)=300\ \mathrm{K} \tag{7}$$

During the femtosecond-to-picosecond time period, it is reasonable to assume that heat losses from gold layer to surrounding as well as to the front surface can be reasonably neglected because of the ultrafast process of the two-temperature relaxation

period compared to that of the irradiation thermal loss cycle. As laser energy diffuses to fused silica, the energy loss to surrounding is also neglected due to the weak temperature perturbance in borderlines of fused silica. Therefore, the boundary conditions can be written as

$$\left.\frac{\partial T_e^I}{\partial n}\right|_{\Omega} = \left.\frac{\partial T_e^I}{\partial n}\right|_{\Omega} = 0 \tag{8}$$

$$\left.\frac{\partial T^{II}}{\partial n}\right|_{\Omega_1} = 0 \tag{9}$$

here, Ω and Ω_1 represent the borderlines contacting with the surrounding of the metal film and fused silica.

At the interface of gold-coated fused silica, the thermal contact is mainly dominated by phonon. So the boundary conditions of the interface can be written as:

$$\left.\frac{dT_e}{dx}\right|_{x=L} = 0 \tag{10}$$

$$\left.T_p^I\right|_{x=L} = \left.T^{II}\right|_{x=L} \tag{11}$$

$$K^I\left.\frac{\partial T^I}{\partial x}\right|_{x=L} - K^{II}\left.\frac{\partial T^{II}}{\partial x}\right|_{x=L} = h\left(\left.T^I\right|_{x=L} - \left.T^{II}\right|_{x=L}\right) \tag{12}$$

Here, h is treated as constant parameter at the normal thermal relaxation process.

Because of the flexibility of finite element method in dealing with the heat transfer equations, the partial differential Eqs. (1) and (2) are simultaneously solved by the Finite Element Method (FEM). In the current FEM simulations, three main steps are employed for the calculation procedures. Firstly, we build the geometrical domain of gold coated fused silica; Secondly, the mesh generation procedure is carried out to divide the geometry into patches. Following that, we introduce the mathematical expression into the meshed geometry, and solving the mathematical expression using FEM procedures package. The initial conditions for electrons and phonons are assumed to be room temperature. During the electron-phonon coupling period, it is reasonable to assume that heat losses from the metal film to the surrounding as well as to the front surface are neglected. During the thermal diffusion relaxation period, the thermal contact is mainly dominated by phonon at the interface of gold coated fused silica. In the current FEM simulations procedures, the geometry is nonlinearly meshed across the laser spot space and the time step size is settled as 5 fs which is smaller than the laser pulse duration for precisely calculating the temporal evolution behavior of the ultrafast thermal excitation in gold-coated fused silica system.

3. Results and discussion

The thermal and optical physical parameters for gold layer and fused silica are listed as follows: gold layer: $g = 2.6 \times 10^{16}$ w/(m^{3}k); $k_0 = 315$ w/(mk); $C_{e0} = 2.1 \times 10^4$ J/(m^{3}k); $C_p = 2.5 \times 10^6$ J/(m^{3}k)); fused silica: $k = 1.38$ w/(mk) [20].

The thickness of gold layer is treated as an adjustable variable and the thickness of fused silica is fixed at 2 μm. The related laser parameters we used are: $\lambda = 800$ nm, $t_p = 30$ fs.

The electron and phonon temperature field distributions along the depth of gold-coated fused silica at different delay time of electron-phonon relaxation and thermal diffusion relaxation periods are shown in Fig. 2. It can be seen from Fig. 2(a) that gold film electrons are obviously perturbed during the electron-phonon relaxation period. However, the fused silica keeps undisturbed on the picosecond timescale. When the delay time is less than 10 ps, indicating the electron and phonon systems are reaching thermal equilibrium, the electron temperature gradient exists in gold layer. However, the electron temperature distributions in gold layer keep almost uniform when the delay time exceeds 10 ps, showing that electrons and phonons have established thermal equilibrium during this period. After 10 ps, the thermal diffusion mechanism will dominate thermal relaxation process in the gold-coated fused silica system. It can be seen from Fig. 2(b) that the phonon temperature is distributed uniformly across the gold layer on the nanosecond timescale during the thermal diffusion period. However, the phonon temperature decays rapidly in fused silica near the interface of gold-coated fused silica system. In current simulations, the fused silica is weakly excited and the thermal conduction in the fused silica is mainly dominated by phonons. Therefore, we name the temperature of fused silica with the phonon temperature of fused silica of T_p. With increase of delay time from 1 ns to 50 ns, the phonon temperature decreases in gold layer, while increases in fused silica, which can be attributed to gold layer energy diffusion into substrate due to phonon–phonon collision across the interface of gold-coated fused silica system.

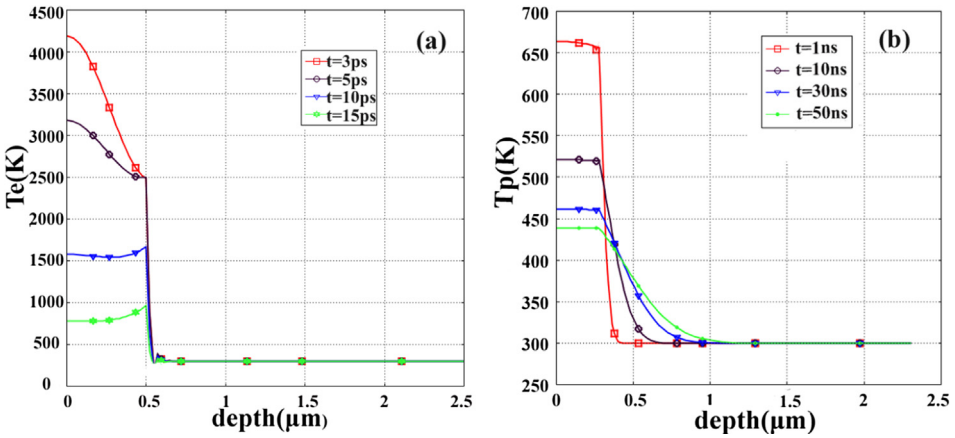

Fig. 2. The electron and phonon temperature field distributions along the depth of gold-coated fused silica at different delay time of electron-phonon relaxation (a) and thermal diffusion relaxation periods (b). The thickness of gold film is 0.5 μm and 0.35 μm, respectively. (For interpretation of the references to color in this figure legend, the reader is referred to the web version of this article.)

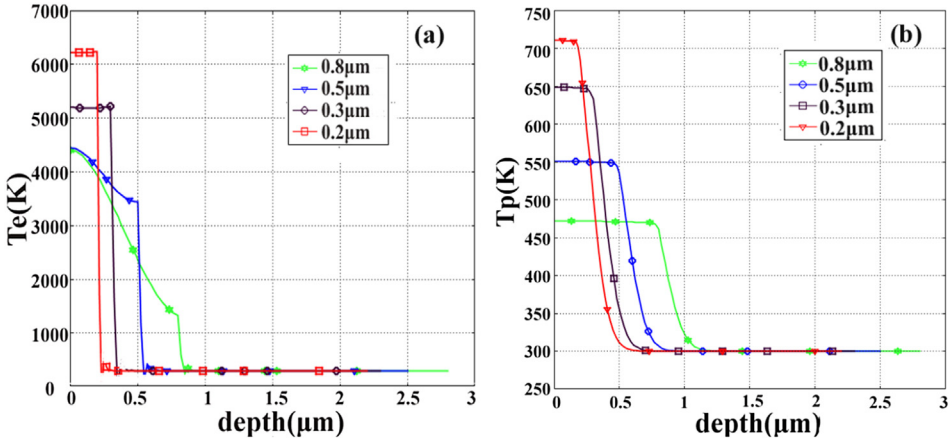

Fig. 3. The electron temperature field distributions at 5 ps (a) and phonon temperature field distributions at 10 ns (b) along the depth of gold-coated fused silica with different gold layer thickness. (For interpretation of the references to color in this figure legend, the reader is referred to the web version of this article.)

The electron temperature field distributions at 5 ps and phonon temperature field distributions at 10 ns along the depth of gold-on-fused silica with different gold layer thickness are shown in Fig. 3. It can be seen from Fig. 3(a) that the electron temperature drops sharply at the interface of gold-coated fused silica but keeps room temperature in fused silica. This is attributed to the fact that the electron thermal energy can be less transferred to fused silica substrate due to nonmetal characteristics of fused silica, in which less free electron can be generated to enhance the thermal conduction with gold layer. It can be seen from Fig. 3(b) that at time of 10 ns during the thermal diffusion period, the gold layer phonon temperature becomes almost uniform and begins to fall near interface of gold-coated fused silica. More interestingly, we can see that phonon temperature is inversely proportional to gold layer thickness across gold-coated fused silica system. This can be interpreted as that at time of 10 ns, the heat energy has uniform distribution in the gold layer, and there is a tiny fraction of heat energy transfer from gold layer to fused silica. Therefore, at the case that the total heat energy is almost the same, the average heat energy in gold layer is inversely proportional to the film thickness.

The maximal phonon temperatures at point A (laser spot center on surface) and point B (laser spot center on interface) of gold-coated fused silica system as functions of gold layer thickness are shown in Fig. 4. We can see that as the thickness of gold layer is less than 0.6 μm, the maximal phonon temperature at point A decreases dramatically with increasing gold layer thickness. Once the thickness exceeds 0.6 μm, the phonon temperature at point A keeps constants with values of 437 K, 524 K, 607 K for three different laser

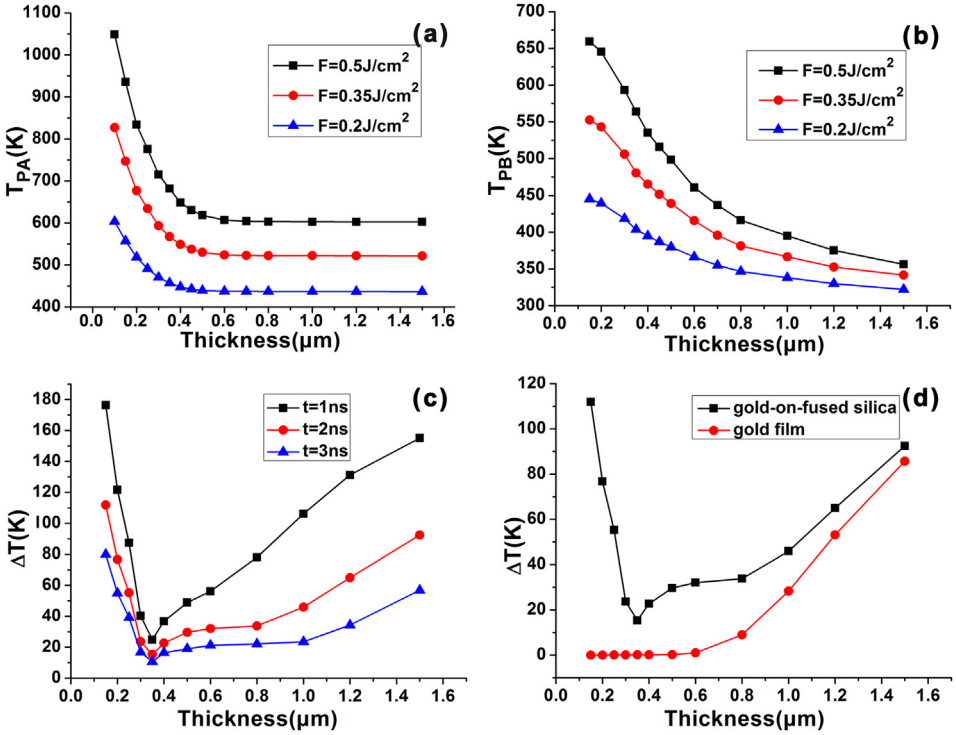

Fig. 4. The dependence of phonon temperature and temperature difference across the gold layer of gold-coated fused silica on gold layer thickness. (For interpretation of the references to color in this figure legend, the reader is referred to the web version of this article.)

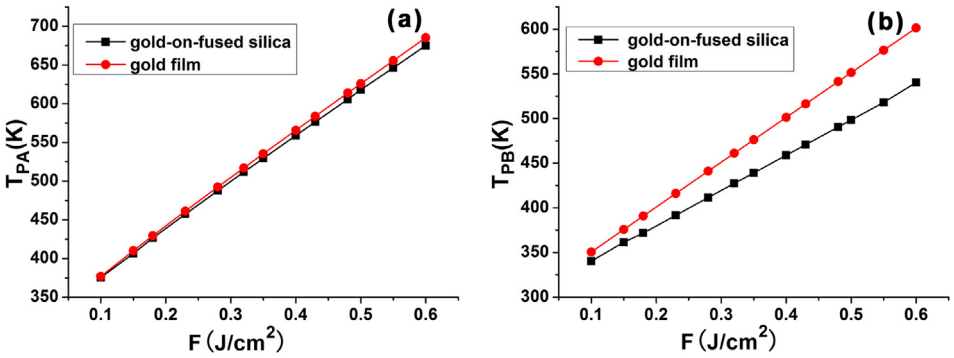

Fig. 5. The maximal phonon temperature field distributions at the different situations that the gold-coated fused silica system and the free gold film structure as a function of laser fluence. (For interpretation of the references to color in this figure legend, the reader is referred to the web version of this article.)

fluence of 0.2 J/cm^2, 0.35 J/cm^2, 0.5 J/cm^2, respectively. The result shows that 0.6 μm is the critical film thickness and the maximal phonon temperature is not affected by the gold layer thickness as it is larger than 0.6 μm. It can be attributed to the critical thermal diffusion length in the gold film, which is calculated to be 0.6 μm during the electron-phonon relaxation period in the current simulations. As the gold film thickness exceeds 0.6 μm, the gold film can be treated as the bulk target. As a result, the maximal surface phonon temperature is not affected by the gold layer thickness as it is larger than 0.6 μm. We can see from Fig. 4(b) that the maximal phonon temperature at point B decreases slowly with increasing of gold layer thickness and the speed of temperature decreases at point B becomes smaller as laser fluence continuously increases. Fig. 4(c) shows the temperature difference (ΔT) of phonon temperature across gold layer of gold-coated fused silica system as a function of gold layer thickness at three different relaxation time. We can see that as the gold layer thickness is less than 0.35 μm, drops dramatically with increasing of gold layer thickness, while ΔT increases slowly once the gold layer thickness exceeds 0.35 μm. It indicates that the thermal loading damage of gold layer due to thermal gradient across gold layer is relatively small when the gold layer thickness approaches 0.35 μm. When the gold layer thickness is less than 0.35 μm, the increasing of the gold film thickness will cause obvious drop of gold layer surface temperature, meanwhile, the temperature at the bottom of gold layer can slightly decrease due to the weak role of the thermal diffusion into the substrate at a few nanoseconds. Therefore, the temperature difference drops dramatically with increasing of gold layer as it is less than 0.35 μm. However, as the gold layer thickness exceeds 0.35 μm, defined as the critical length corresponding to the distance from the surface of gold layer to the thermal wave front center. The increasing of the gold layer thickness will cause weakening of the thermal wave front energy arriving at the interface, leading to decrease of the temperature at the interface. Meanwhile the temperature of gold layer surface can be slightly affected by the interface resistance as the gold layer thickness exceeds 0.35 μm at a few nanoseconds. Therefore, the temperature difference increases slowly with increasing gold layer thickness as it exceeds 0.35 μm. We compared the temperature difference of the phonon temperature across the gold film of the free-standing gold film and gold-coated fused silica system (Fig. 4(d)). It shows as the gold film thickness is less than 0.6 μm, the temperature difference ΔT differs greatly for the free-standing gold film and gold-coated fused silica system. Once the gold layer thickness exceeds 0.6 μm, the temperature difference exhibits a similar tendency for free-standing gold film and gold-coated fused silica system. It indicates that gold layer thickness of 0.6 μm is the critical thickness and once the gold layer thickness is less than 0.6 μm, the substrate will significantly impact on phonon temperature distribution of gold layer. However, the phonon temperature distribution can be less affected by the interface of gold-coated fused silica as gold layer thickness exceeds 0.6 μm. This conclusion should be basically beneficial for understanding processes of ultrafast thermalization dynamics in gold-coated fused silica system for well optimizing femtosecond laser microfabrication of the composite structures system.

The maximal phonon temperature at point A (laser spot center on surface) and point B (laser spot center on bottom of gold layer) as a function of laser fluence for free-standing gold film and gold-coated fused silica system are shown in Fig. 5. It can be seen from Fig. 5(a) that the maximal phonon temperature at point A presents almost linear grows with increasing laser fluence and exhibits less difference for gold-coated fused silica system and free-standing gold film. We can see from Fig. 5(b) that the maximal phonon temperature at point B also grows linearly with increasing laser fluence. More importantly, the temperature difference between gold-coated fused silica system and free-standing gold film becomes more and more obvious with increasing laser fluence. The results indicate that the fused silica substrate can significantly affects the phonon thermalization of at the bottom of gold film, but less affects the thermalization of on the gold film surface.

4. Conclusion

In this paper, we numerically investigated the ultrafast thermalization dynamics of gold-coated fused silica system. The results indicate that the thermal loading damage of gold layer due to thermal gradient across gold layer is relatively small when the gold layer thickness approaches 0.35 μm. As the gold layer thickness is less than 0.6 μm, the fused silica substrate will significantly impact on phonon temperature distribution of gold layer. The results should be basically helpful for understanding the fundamental thermalization processes of gold-coated fused silica system for well optimizing laser micro-and nano fabrication.

Acknowledgements

This work is supported by the National Science Foundation of China under the Grant Nos. 51335008, 61275008 and 61176113, the Special-funded programme on National Key Scientific Instruments and Equipment Development of China under the Grant No. 2012YQ12004706.

References

[1] N. Leng, L. Jiang, X. Li, C. Xu, P. Liu, Y. Lu, Appl. Phys. A 109 (2012) 679–684.
[2] W. Watanabe, N. Arakawa, S. Matsunaga, T. Higashi, K. Fukui, K. Isobe, K. Itoh, Opt. Express 12 (2004) 4203.
[3] K. Furusawa, K. Takahashi, H. Kumagai, K. Midorikawa, M. Obara, Appl. Phys. 69A (1999) 359.

[4] J.K. Chen, W.P. Latham, J.E. Beraun, J. Laser Appl. 17 (2002) 63.
[5] E.T. Swartz, R.O. Pohl, Rev. Mod. Phys. 61 (1989) 605.
[6] P.E. Hopkins, P.M. Norris, Appl. Surf. Sci. 253 (2007) 6289.
[7] P.E. Hopkins, J.L. Kassebaum, P.M.J. Norris, Appl. Phys. 105 (2009) 023710.
[8] G. Liang, Stephen L. Hodson, J. Heat Transf. 1 (2012).
[9] G. Du, F. Chen, Q. Yang, J. Si, X. Hou, Opt. Commun. 284 (2011) 640.
[10] G. Du, F. Chen, Q. Yang, J. Si, X. Hou, Opt. Commun. 283 (2010) 1869.
[11] J. Wang, C. Guo, J. Appl. Phys. 102 (2007) 053522.
[12] O.W. Käding, H. Skurk, K.E. Goodson, Appl. Phys. Lett 65 (1994) 1629.
[13] Arun Majumdar, Pramod Reddy, Appl. Phys. Lett. 844 (2004) 768.
[14] M. Bonn, N.D. Denzler, S. Funk, M. Wolf, S.S. Wellershoff, J. Hohlfeld, Phys. Rev. B 61 (2000) 1101.
[15] L. Jiang, H.L. Tsai, Int. J. Heat. Mass Transf. 50 (2007) 3461.
[16] A.P. Kanavin, I.V. Smetanin, V.A. Isakov, Yu.V. Afanasiev, B.N. Chichkov, B. Wellegehausen, S. Nolte, C. Momma, A. Tünnermann, Phys. Rev. B 57 (1998) 14698.
[17] J.P. Colombier, P. Combis, F. Bonneau, R. Le Harzic, E. Audouard, Phys. Rev. B 71 (2005) 165406.
[18] L. Jiang, Hai-Lung Tsai, J. Appl. Phys. 104 (2008) 093101.
[19] P.B. Allen, Phys. Rev. Lett. 59 (1987) 1460.
[20] A.M. Chen, H.F. Xu, Y.F. Jiang, Appl. Surf. Sci. 257 (2010) 1678.
[21] A.A. Unal, A. Salmashonak, G. Seifert, H. Graener, Phys. Rev. B 79 (2009) 115411.
[22] H.P. Chen, Y.C. Wen, Y.H. Chen, Appl. Phys. Lett. 97 (2010) 201102.